Initial spreading of a mega feeder nourishment: Observations of the Sand Engine pilot project

Matthieu A. de Schipper [a,b,*], Sierd de Vries [a], Gerben Ruessink [c], Roeland C. de Zeeuw [b], Jantien Rutten [c], Carola van Gelder-Maas [d], Marcel J.F. Stive [a]

[a] Faculty of Civil Engineering and Geosciences, Department of Hydraulic Engineering, Delft University of Technology, Delft, The Netherlands
[b] Shore Monitoring and Research, The Hague, The Netherlands
[c] Faculty of Geosciences, Department of Physical Geography, Utrecht University, Utrecht, The Netherlands
[d] Ministry of Infrastructure and the Environment (Rijkswaterstaat), Lelystad, The Netherlands

ARTICLE INFO

ABSTRACT

Sand nourishments are a widely applied technique to increase beach width for recreation or coastal safety. As the size of these nourishments increases, new questions arise on the adaptation of the coastal system after such large unnatural shapes have been implemented. This paper presents the initial morphological evolution after implementation of a mega-nourishment project at the Dutch coast intended to feed the surrounding beaches. In total 21.5 million m³ dredged material was used for two shoreface nourishments and a large sandy peninsula. The Sand Engine peninsula, a highly concentrated nourishment of 17 million m³ of sand in the shape of a sandy hook and protruding 1 km from shore, was measured intensively on a monthly scale in the first 18 months after completion. We examine the rapid bathymetric evolution with concurrent offshore wave forcing to investigate the feeding behaviour of the nourishment to the adjacent coast. Our observations show a large shoreline retreat of O (150 m) along the outer perimeter of the peninsula, with locally up to 300 m retreat. The majority (72%) of the volumetric losses in sediment on the peninsula (1.8 million m³) were compensated by accretion on adjacent coastal sections and dunes, confirming the feeding property of the mega nourishment. Further analyses show that the morphological changes were most pronounced in the first 6 months while the planform curvature reduced and the surf zone slope flattened to pre-nourishment values. In the following 12 months the changes were more moderate. Overall, the feeding property was strongly correlated to incident wave forcing, such that months with high incoming waves resulted in more alongshore spreading. Months with small wave heights resulted in minimal change in sediment distribution alongshore and mostly cross-shore movement of sediment.

1. Introduction

Sand nourishments are nowadays widely applied to enhance coastal safety and to increase beach width (e.g. Burcharth et al., 2015; Castelle et al., 2009; Dean, 2002; Kuang et al., 2011; Luo et al., 2015; Ojeda et al., 2008; Roberts and Wang, 2012; Yates et al., 2009). With the increasing pressure on the coastal zone in terms of population and the (projected) relative sea level rise, the number of nourishment projects and the total volume has increased greatly, e.g. for the US East Coast alone Valverde et al. (1999) report an increase in annual nourishment volume over all projects combined from ~1 10⁶ m³/year in the 1920s

to ~12 10⁶ m³/year in the 1990s. The first nourishment projects, executed roughly before the 1970s, targeted specific local weak spots along the coast (Hanson et al., 2002; Valverde et al., 1999). The added sand was mostly placed on dunes or beaches and the success rate of the nourishment was predominantly quantified by the proportion of material remaining in the project area over time (e.g. Elko and Wang, 2007; Leonard et al., 1990). The cross-shore size of these nourishments, i.e. the nourished volumes per meter alongshore, was typically small (order of 100 m³ per m) if these were used for beach maintenance. Following up on these initial beach and dune nourishments, shoreface nourishments have been carried out in the last quarter of the 1900s as an economical alternative for some locations (Grunnet and Ruessink, 2005; Mulder et al., 1994; Niemeyer et al., 1996). The cross-shore size of these nourishments is typically larger, i.e. in the order of 400–600 m³/m (e.g. Ojeda et al., 2008; van Duin et al., 2004). The positive effect of a shoreface nourishment on the beach and dunes can be subdivided into two hypothesized effects: the wave attenuation

* Corresponding author.
 E-mail addresses: M.A.deSchipper@TUDelft.nl (M.A. de Schipper), SierddeVries@TUDelft.nl (S. de Vries), B.G.Ruessink@uu.nl (G. Ruessink), Roeland@shoremonitoring.nl (R.C. de Zeeuw), J.Rutten@uu.nl (J. Rutten), Carola.van.Gelder-Maas@rws.nl (C. van Gelder-Maas), M.J.F.Stive@tudelft.nl (M.J.F. Stive).

function and the (cross-shore) feeder function (Mulder et al., 1994). The wave attenuation function is formed as waves break on the nourishment during storm conditions, thus reducing the wave energy and longshore wave driven currents higher up the profile. The second, feeder effect is caused as a gradual landward movement of sand is stimulated, thus causing a seaward movement of the coastline. Although in practice it can be difficult to delineate between both effects, measurements (Hoekstra et al., 1996) and modelling (van Duin et al., 2004) of experimental nourishments suggest that both effects are present.

At present, sandy mitigation strategies using frequent (every 3 to 10 years) beach and shoreface nourishments are carried out as the solution for several populated sandy coasts with a structural coastal recession (Cooke et al., 2012; Hamm et al., 2002). For locations with a large annual sand deficit however large quantities of sand need to be supplied or frequent re-nourishments are needed. It is questionable whether such frequent re-nourishing has not a detrimental effect on the fauna of the nourished site (e.g. Janssen et al., 2008; Peterson and Bishop, 2005; Speybroeck et al., 2006). Such potential negative effects and the upscaling to a more regional approach have given the incentive to look for better methods. In this light, the concept of nourishing with the intention to feed adjacent coasts by means of alongshore diffusion in the form of concentrated (mega) nourishments have been proposed as an alternative (Stive et al., 2013). In this approach a large volume of sand is placed at a single location with the intention to feed a larger alongshore stretch of coast over time. Under the combined natural forces of wind, waves and tides the sediment is expected to be redistributed in along and cross-shore directions, hence enhancing the safety of a longer stretch of coast. In the Netherlands, a concentrated mega-scale nourishment called the Sand Engine was implemented in 2011 as a large sandy hook with the size of approximately 17 million m^3 placed in an area of 2.5 km in the alongshore direction and 1 km in the cross-shore. In contrast to previous nourishments with cross-shore sizes of 400–2000 m^3 per meter alongshore and small transitions with the surrounding coastlines, the Sand Engine peninsula design project has a highly concentrated nourishment volume (up to 10.000 m^3/m) and sharp coastline angles with the intention to

redistribute rapidly by means of alongshore diffusion of sand. An evaluation of such a feeder nourishment project cannot solely done in terms of the amount of sand that remains within the project area (as done with more traditional nourishments; e.g. Dean and Yoo, 1992; Elko and Wang, 2007; Verhagen, 1996), but requires a broader view on the coastal section, including the rate of spreading and the magnitude of the accumulation of sediment on adjacent coastal sections.

The objective of the current paper is to present the morphological evolution of the Sand Engine in the first 18 months after construction. Special attention is on the feeding character of the nourishment, assessing spatial and temporal redistribution of sediment. Although it is known that this response in the first period after completion is vital for the total evolution of the project, it is often poorly recorded due the lack of frequent monitoring data (Elko and Wang, 2007). We performed a high resolution monitoring study with frequent surveys to capture this behaviour in the first period after completion. In this paper we discuss the feeding of the mega nourishment pilot by focusing on the planform adjustment of the nourished peninsula (Section 4.2), cross-shore profile and volume changes at the Sand Engine and along adjacent coasts (Section 4.2), quantifying the proportion of eroded sand on the peninsula with respect to the accretion on adjacent sections (Section 4.3) and relating the feeding behaviour on a monthly timescale to the incoming wave power and the shape of the peninsula (Section 4.4).

2. The Sand Engine project

2.1. Coastal setting

The Sand Engine nourishment was executed along the 'Westland' coastal cell, a 17 km stretch of coast between the harbour entrances of Scheveningen and Rotterdam (Fig. 1). This southern part of the Dutch coast is subject to structural erosion, the coastline migrated landward by about 1 km in the period 1600–1990. After a retreat of O (300 m) in the 18th century, construction of rubble mound groynes was initiated (van Rijn, 1997). Yet, as this coastal stretch remained erosive despite the
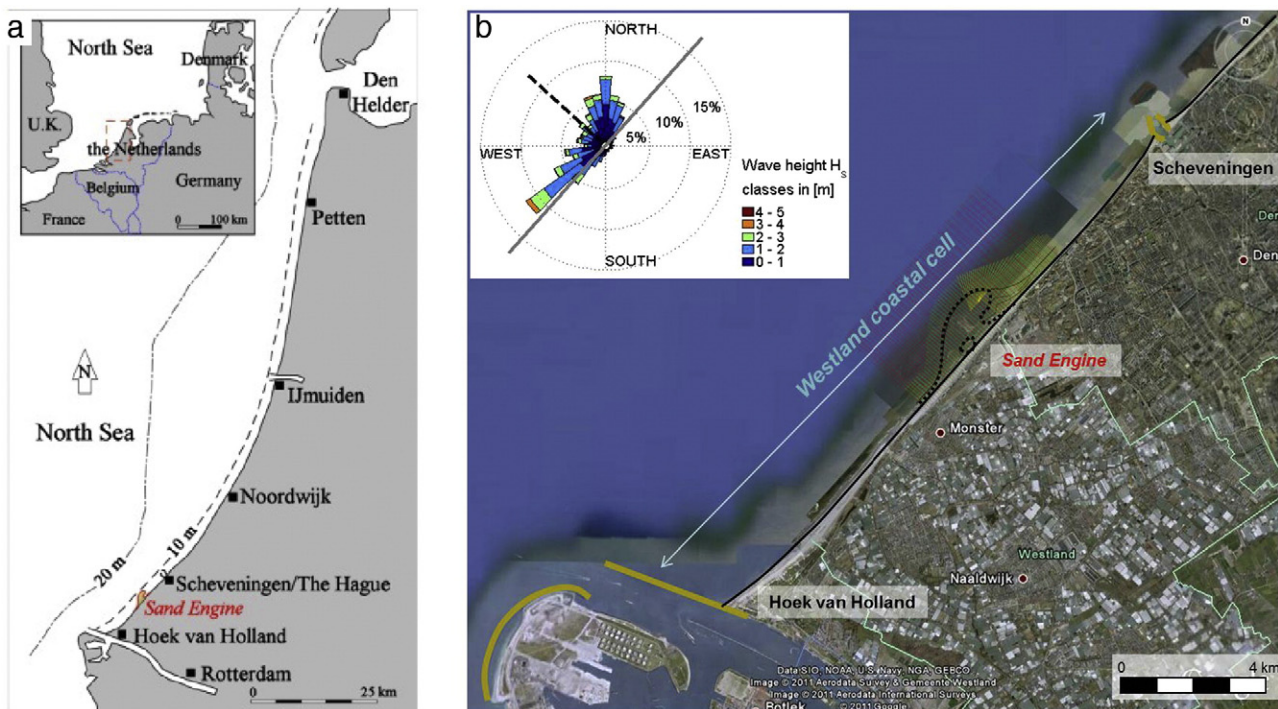

Fig. 1. a) Location of the Sand Engine on the North Sea coast. b) The 17 km Westland coastal cell in between the harbour entrances (represented by the yellow lines) of Scheveningen and Hoek van Holland. The insert shows the wave rose based on four years of data at Europlatform. Image data: Google, Aerodata.

groynes sand nourishments were introduced as mitigation measure in the 1970s. Since then, nourishments have been implemented more frequently, especially from 1990 onwards when the implementation of the 'Dynamic Preservation Act' dictated that the 1990 coastline position had to be maintained at all costs (van Koningsveld and Mulder, 2004). At the site of the Sand Engine, the first nourishment was implemented in 1986. Since then it has been re-nourished eight times prior to the construction of the Sand Engine. In all, approximately 55 million m^3 of sand was added until present to the 17 km Westland coastal cell for mitigation of erosion and land reclamation. In the last years the nourishment volumes in this stretch have increased to ~1.7 10^6 m^3 per annum (~100 m^3/m alongshore/year). The net yearly-averaged alongshore sediment transport in the middle of the Westland coastal cell is estimated to be 3.8 10^5 m^3 northward excluding pores, resulting from the gross transports in both directions, i.e. 7.6 10^5 m^3 northward and 3.8 10^5 m^3 southward (van Rijn et al., 1995).

Prior to the Sand Engine pilot project the beach was O (150) m wide with a mild lower shoreface slope (1:300) (Fig. 1a). The median grain size around the shoreline in this area is O (250 μm) (Wijnberg, 2002). The slope of the profile in the intertidal and surfzone (+1 to −4 m) prior to all the nourishment works (averaged over 1965 to 1985) was 1:55 in this coastal stretch. The profile on the Holland coast generally contains multiple nearshore subtidal bars, migrating offshore in cycles with return intervals of 4 to 16 years (Ruessink et al., 2003). At the Westland coastal cell however only a single bar offshore of the groyne heads was observed (Wijnberg and Terwindt, 1995) without a net annual migration. Possibly the less prominent bar behaviour and cyclic migration at this site was influenced by the presence of the groynes. Near the waterline a seasonal pattern is present in the beach width and the cross-shore volume of the supra tidal beach, related to the seasonality in the wave forcing (Quartel et al., 2008).

The southern Dutch coast faces the shallow (20–80 m deep) North Sea basin, and as a result the wave climate is wind sea dominated with annual mean wave height H_s of 1.3 m and wave periods typically in the order of 5–6 s (Wijnberg, 2002). Energetic storm events in autumn and winter are often from the south-west and north, causing
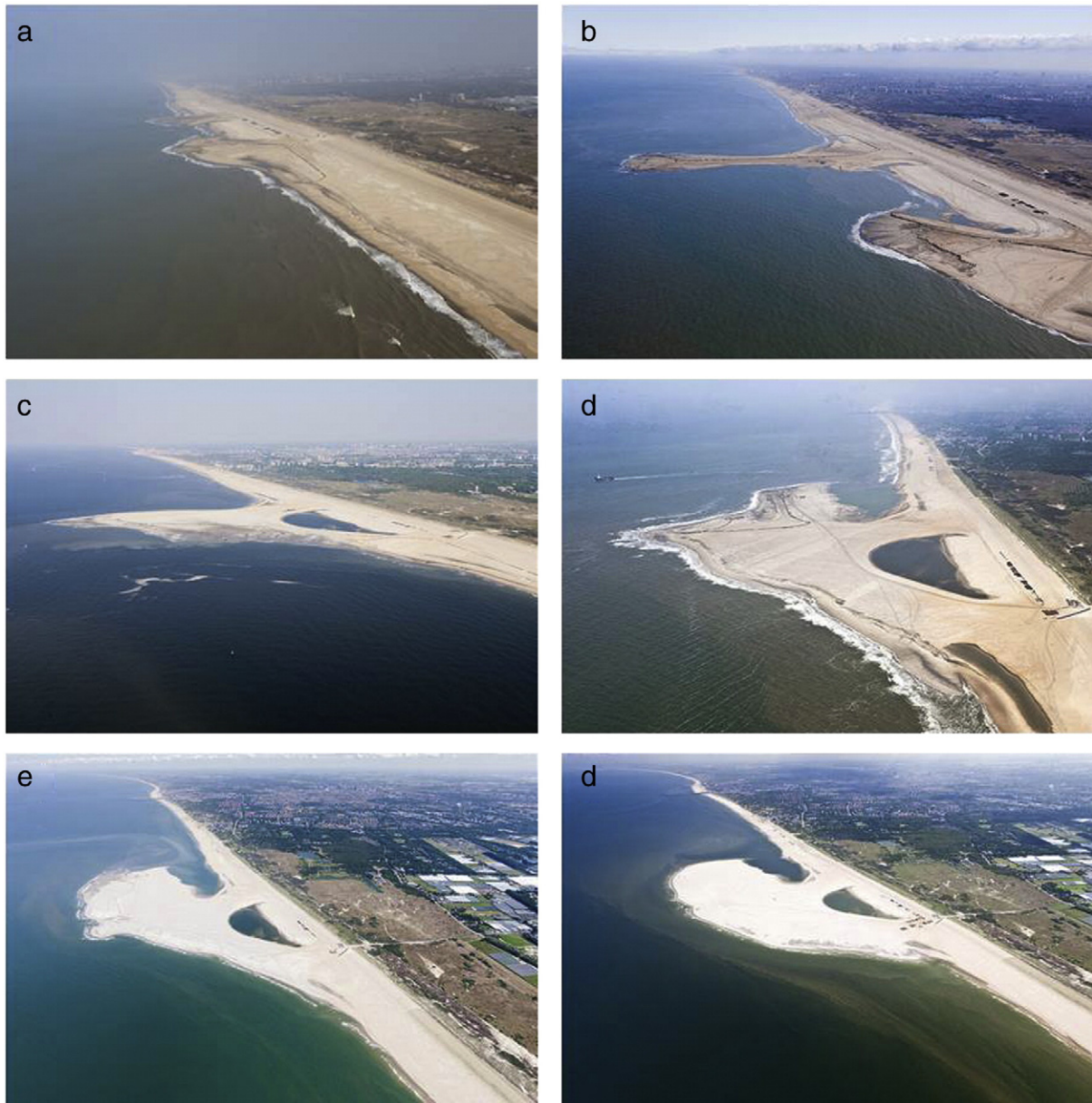

Fig. 2. Aerial photographs of the Sand Engine project during construction on a) March 15, b) March 25, c) April 25, d) May 17, e) June 14 and f) July 11, 2011 shortly after completion of the peninsula. Image data: Rijkswaterstaat/Joop van Houdt.

wave incidence to be highly oblique. Storms with a return period of once in a year have a significant wave height offshore of about 4 m. The mean tidal range at the location of the Sand Engine is 1.7 m and the horizontal tidal velocities have an amplitude of O (0.5 m/s).

2.2. The Sand Engine nourishment

The Sand Engine project consists of a mega nourishment peninsula and two flanking shoreface nourishments with a total dredged sediment volume of 21.5 million m³. The main part, the mega nourishment, was shaped as a large hook-shaped peninsula with the outer tip curved towards the north (Fig. 2). This design fulfilled best the multi-disciplinary requirements of safety in combination with living quality and innovation (Stive et al., 2013). Early predictions of the development of the peninsula suggested lee side erosion on both sides; two flanking shoreface nourishments were proposed to mitigate this effect (Deltares, pers. comm.). About 19 million m³ of dredged sediment

was planned for the curved peninsula, with 2 million m³ and 0.5 million m³ for the northern and southern additional shoreface nourishments respectively. The present paper focuses on the evolution of the peninsula and the term Sand Engine is from hereon used to indicate the peninsula only.

In the design of the Sand Engine the most seaward position of the shoreline was foreseen to protrude ~1000 m from the original shoreline. The cross-shore slope of the peninsula was 1:50, such that the toe of the nourishment was at −8 m and 1500 m from the original shoreline. The alongshore footprint of the Sand Engine peninsula was planned to be 2000 m. In the design, the tip of the peninsula was curved northward creating a sheltered area that was intended to be a nurturing ground for ecology (Fig. 2f). Furthermore, the design contained a small (~8 ha) lake at the base of the peninsula (see Fig. 2f). This lake was intended to prevent the freshwater lens in the dunes to migrate seaward, which could endanger the water extraction from the more landward dune area.
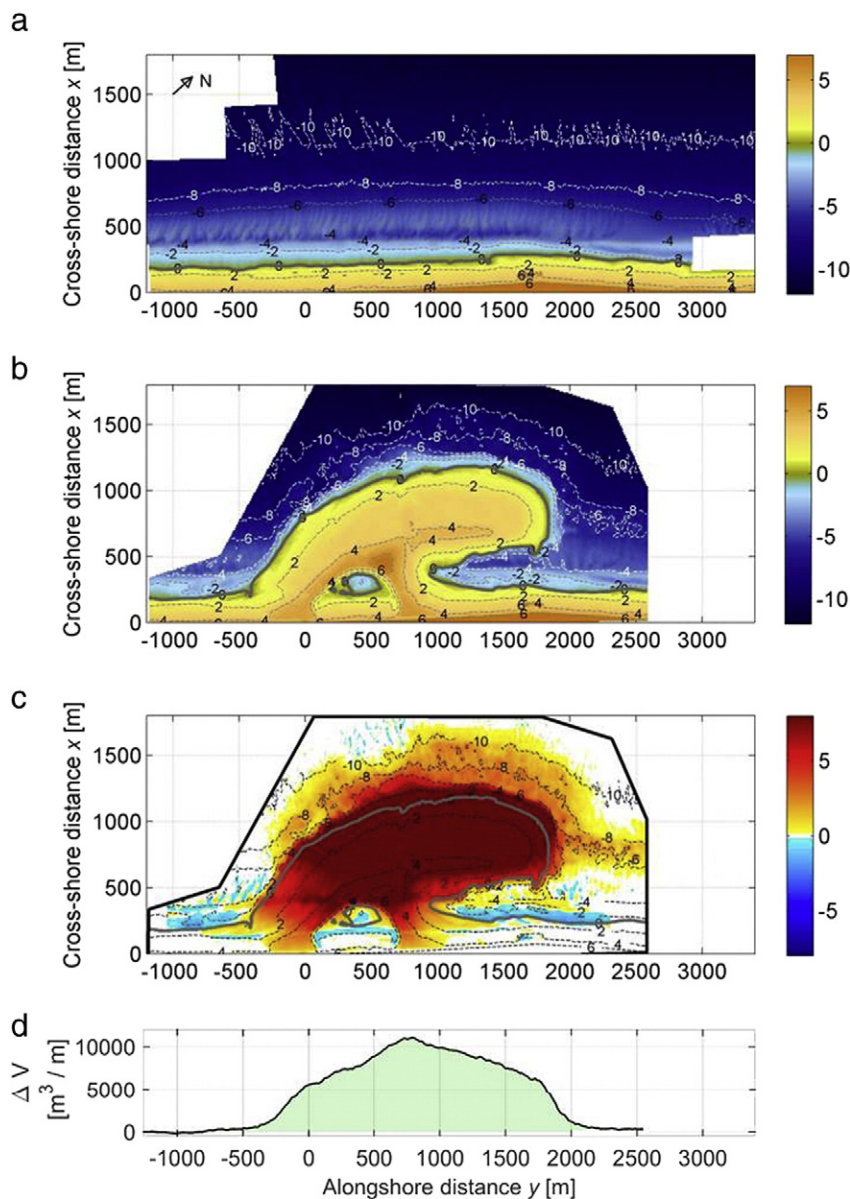

Fig. 3. Bed elevation data a) prior and b) post construction of the Sand Engine peninsula. Colours show the bed elevation in meters with respect to the NAP datum (approximately MSL). Data are shown in a local, shore-orthogonal coordinate system. Panel c) presents the difference in bed level in meters between surveys prior and post construction, highlighting the added volume. Bed level changes smaller than ± 10 cm are omitted. The black line indicates the border of the area covered by both surveys. Contour lines indicate the post construction bed elevation, with the 0 m NAP contour highlighted by the thick dashed line. Panel d) shows the profile integrated volume difference ΔV between both surveys.

The construction of the Sand Engine took place from March 2011 to July 2011 (Fig. 2). The Sand Engine was constructed using trailing-suction hopper vessels, used to either dump or spray sand in intermediate waters or to pump sand ashore. The construction started with the building of a narrow cross-shore seaward dam, such that alongshore losses from this initial build out would remain within the project domain as much as possible. The outer rim of the peninsula was completed last (Fig. 2e, f). The sediment for the nourishment was dredged 5 to 10 km offshore of the site and was prescribed to be of similar properties to the surrounding coast. Regular grain size analysis during construction (after each 0.5 million m^3 of nourished sediment) showed an average D_{50} of 281 μm.

The bed elevation data were measured prior and after construction of the peninsula by the dredging contractor (Fig. 3a, b). The plan view topographies displayed in Fig. 3 were based on multiple surveys on different dates, and thus do not provide a perfect snapshot of the topography and bathymetry at a single instant. However, the difference between both topographies (Fig. 3 c) highlights the large quantity of added sediment after the implementation of the nourishment. The added volume per profile is an order of magnitude larger than regular nourishments at this part of the coast, exceeding 1.10^4 m^3 per m alongshore near the most seaward point of the Sand Engine (Fig. 3 d). By integration over the common areas of both surveys an added volume of 17.02 million m^3 was found in situ, of which 4.04 million m^3 (24%) was located above 0 m NAP (NAP being the Dutch datum at ~ MSL). This added volume based on surveys was O (10%) smaller than the 19 million m^3 of dredged sediment that was transported for the curved peninsula, due to the losses during construction. After construction the highest point on the Sand Engine peninsula was 7.3 m above NAP, just seaward of the small lake (Fig. 3 b).

3. Methodology

3.1. Post-construction morphology measurements

Following the completion of the peninsula in July 2011, an intensive monitoring programme was initiated. As part of this monitoring programme, the area around the Sand Engine peninsula has been surveyed nearly monthly to capture and investigate the adaptation to the large intervention. Surveys span the beach and shoreface area from the dunefoot (~ + 5 m NAP) to beyond the − 10 m NAP contour. The surveyed domain was 4.7 by 1.6 km in along- and cross-shore direction, respectively. The transect grid consists of 59 full cross-shore transects with an average alongshore spacing of 80 m (Fig. 4, red lines). The transect definition for these transects was identical to the so-called 'JARKUS' high-density profiles used for the annual surveys executed by the Dutch

Ministry of Infrastructure and Environment (e.g. Wijnberg and Terwindt, 1995). In the nearshore region the transect distance has been refined with 68 shorter transects to obtain an alongshore transect spacing of O (40 m) on dynamic parts of the beach and surfzone. Furthermore, additional alongshore transects and oblique transects were measured on the northern side of the peninsula to capture the evolution of the lagoon entrance.

Surveys were executed using three different techniques, all based on the real-time kinematic differential global positioning system (RTK-DGPS) surveying technique. Sub-aerial parts were measured using the GPS system mounted on a 4WD quad bike (Fig. 5a). For the sub-aqueous parts of the transects the GPS was mounted on a waverunner/jetski and combined with single beam echo sounder (Fig. 5b). Runnels and narrow tidal channels with small water depth were surveyed using the GPS mounted on a wheeled pole (Fig. 5c). The vertical accuracy of the bed elevation measurements was of order 5, 10 and 3 cm for the three different techniques respectively (Huang et al., 2002; Ruggiero et al., 2009; van Son et al., 2010). The surveys of the full domain were executed during 3 days of calm conditions approximately every month.

To facilitate the analysis of cross- and alongshore displacements, the bed elevation data were rotated to a local shore-orthogonal coordinate system with its origin at the beach entrance 'Schelpenpad'. The collected x, y, z point data of all three survey platforms were combined and interpolated to a 10 by 10 m grid by means of linear interpolation. The resulting 17 bathymetries are depicted in Fig. 6. The monthly surveyed bed elevation data do not incorporate the dune face and first dune row. To estimate the sediment volume loss towards the dunes biannual Lidar flights of the sub-aerial domain were used. These Lidar data were available for July 2011, May 2012, October 2012 and May 2013 and sampled on a 5 by 5 m grid.

3.2. Post-construction process measurements

Concurrent wave height $H_{s,0}$, direction θ_0 and period $T_{m02,0}$ offshore in the months after construction were obtained from a wave station ('Europlatform') located 40 km offshore at a water depth of 32 m (Fig. 7). The wave height has a seasonal signal with the highest waves from September to December (Northern Hemisphere autumn). The high-energy wave events after construction were mostly from the south and west sectors, similar to the long term averaged wave climate (Wijnberg, 2002). The maximum recorded daily-averaged offshore wave height over first 17 months was 4.4 m during the storm on January 5, 2012 (Fig. 7a). In contrast, during summer months wave heights were low, with the lowest average wave height $H_{s,0}$ over a period between two surveys being 0.7 m.
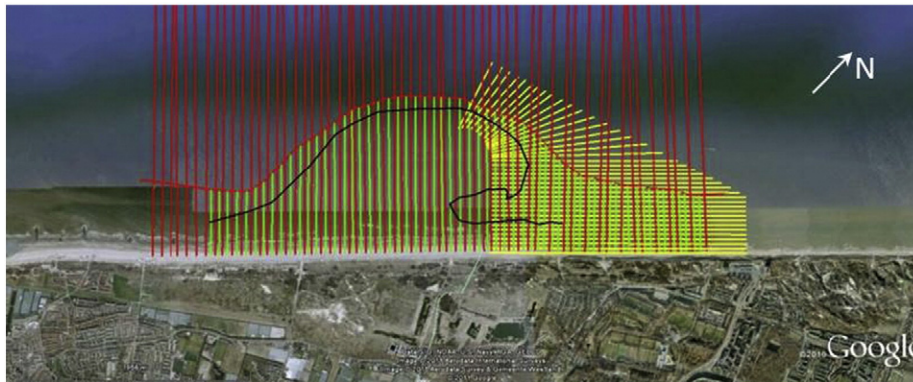

Fig. 4. Surveyed transects projected on an aerial image of the coast prior to construction. Black line indicates the Sand Engine outline after completion of the peninsula. Red lines show the cross-shore transects based on the 'JARKUS' line definitions, yellow lines the supplementary survey transects to capture the detailed morphology in the nearshore (≥ − 6 m NAP). Image data: Google, Aerodata.

Fig. 5. Survey methods applied for the bed elevation measurements of the Sand Engine. a) Quad bike with RTK-GPS, b) survey jetski and c) RTK-GPS on a wheeled pole.

4. Results

4.1. General observations

An overview of the morphological development is given in Fig. 6 and illustrates a rapid, predominantly alongshore redistribution of

sediment. The initial sharp angle in the shoreline on the southern side of the peninsula accreted over time, resulting in a more gradual transition between the nourishment and the adjacent coast (near alongshore location $y = -500$ m, Fig. 8a). The accretion in this transition zone was primarily in the inter- and subtidal zone (between the -6 m and $+2$ m NAP) resulting in a 250 m wide barred inter-tidal zone. The limited
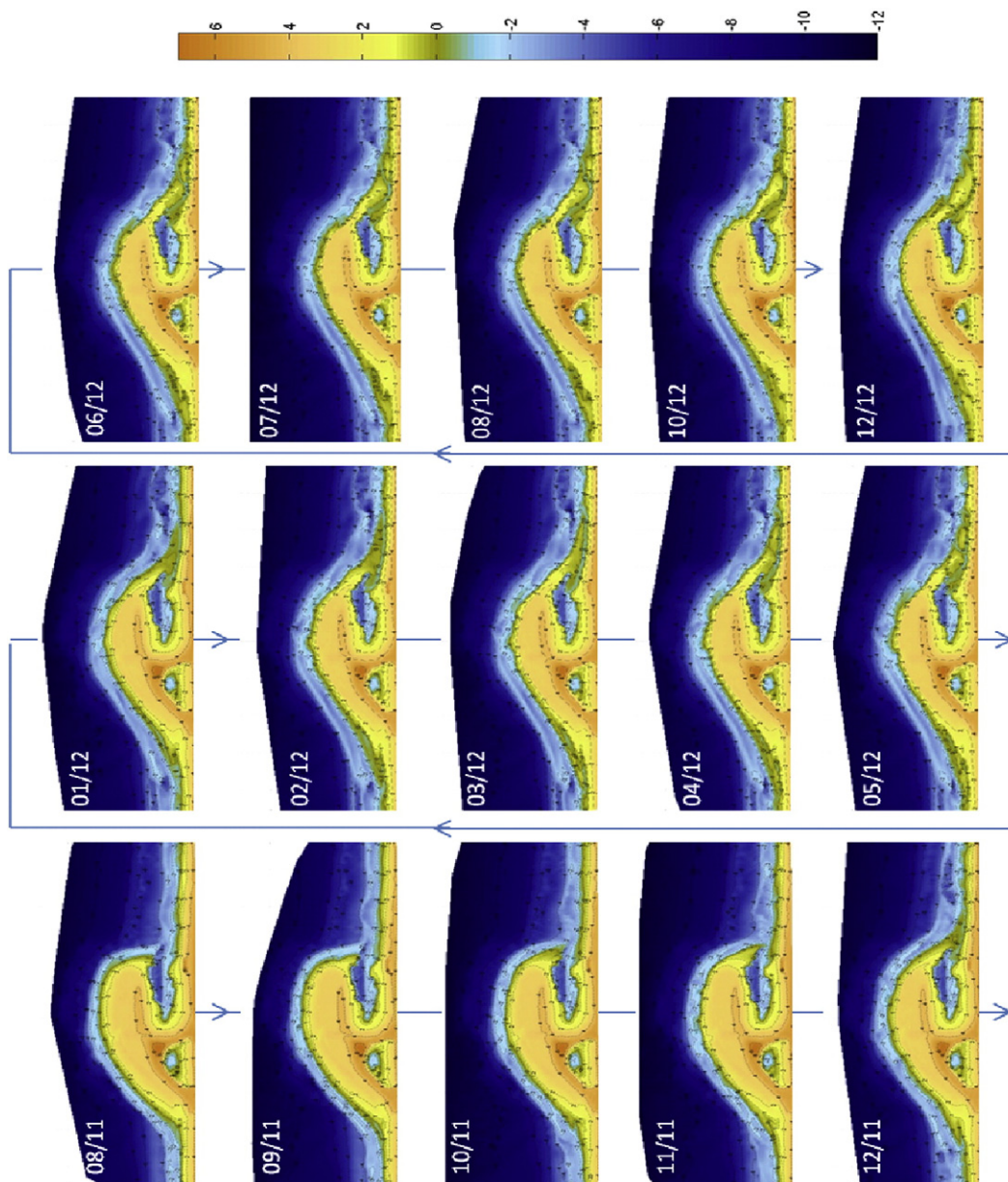

Fig. 6. Measured bed elevation (in meter NAP) of the Sand Engine peninsula in the first 17 months after completion. Every plot shows a domain of approximately 4.7 by 1.6 km in alongshore and cross-shore direction.
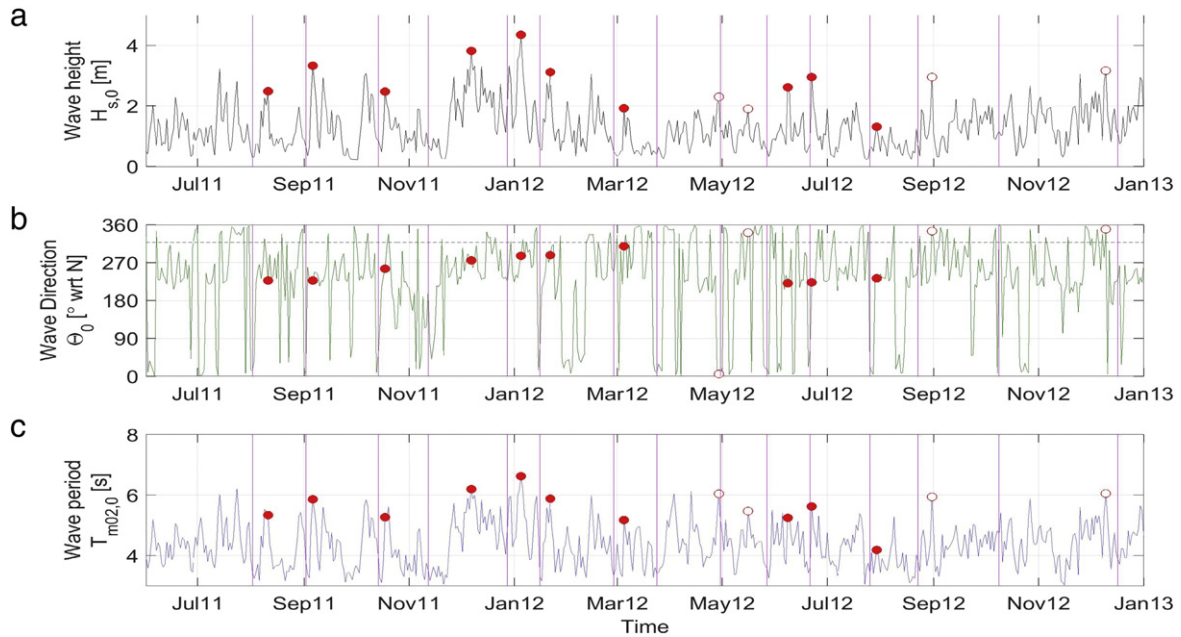
Fig. 7. Daily averaged wave conditions at the Europlatform station versus time. a) Wave height $H_{s,0}$, b) wave direction θ_0 and c) mean wave period $T_{m020,0}$. Pink vertical lines represent survey dates. The horizontal dashed line in panel b) shows the approximate shore normal of the coast prior to the installation of the Sand Engine. Red circles highlight the day with the largest wave height between consecutive surveys, with open and filled symbols for peak wave events coming from the North and South respectively.

change above the +2 m contour suggests that the shape transition was primarily due to marine processes.

On the opposite (northern) side of the peninsula the lagoon entrance dynamics dominated the morphological behaviour. Soon after the implementation of the peninsula a (small) spit-like feature developed, pinching the lagoon entrance over the following months (Fig. 6). In the first 4 to 5 months, this spit mostly elongated in the cross-shore direction towards the adjacent coast and in a later stage it elongated to become a large inter-tidal shoal of 300–400 m across (Fig. 8b). The widening of the spit can be attributed to a seaward expansion but also to a landward widening. The maximum elevation of the spit and shoal were slightly below the high water level, such that they flooded during high tide (and storms). The channel landward of the shoal discharged the flow into and from the lagoon and strong flow velocities of over 1 m/s were observed here during rising and falling tide in the spring of 2012. This channel contained medium 3-D sub-aqueous dunes of O (1 m) length and O (0.5 m) height, similar to those found in tidal channels (Ashley, 1990). As the shoal migrated landward, this channel was forced slightly into the existing beach, similar to the behaviour observed with ebb tidal shoal bypassing (Cheung et al., 2007; FitzGerald, 1982). Towards the end of the investigated period the channel started to meander causing a steep embankment in outer bends.

The largest morphological changes (>0.5 m) over the total period were restricted to the zone −7 to +3 m NAP (Fig. 8c), which gives an indication of the closure depth on these time scales. Small accretion zones can be discerned on the seaward edges of the small lake at the interior of the peninsula and the lagoon. These are thought to be due to eolian sediment transport under influence of the (predominantly) western winds and the large bare sandy surface area upwind of these regions.

4.2. Planform adjustment

The large morphological changes after installation of the peninsula resulted in a transformation of the shape of the artificial peninsula and a reduction of the curvatures along the perimeter (Fig. 8). These changes in the planform shape were quantified by examining the shoreline, which was taken as the most seaward cross-shore position of the 0 m

NAP isobath, $x_{0m}(y)$. The remaining shoreline expansion was quantified by $x_{0m}(y)$ with respect to the 0 m NAP isobath measured prior to construction, $x_{0m,pre}(y)$. To avoid disturbances from smaller scale topographic features (e.g. ridge runnels and swash bar rip channels) a 5 point (i.e. a 50 m) running average filter was applied to $x_{0m}(y)$. The resulting planform contour is shown in Fig. 8 for the first and last survey, and the temporal evolution is displayed in Fig. 9a.

From August 2011 to the December 2012 the maximum cross-shore extent of the Sand Engine reduced by 132 m, i.e. from 906 m to 773 m (~15% decrease). Most of the locations along the outer perimeter of the peninsula (alongshore locations −100 to 1800 m) were subject to retreat of O (150 m) as shown in Fig. 9a. Larger values were found near the northern edge of the peninsula (alongshore $y = 1800$ m) where the initial coastline curvature was the strongest. At this location the 0 m NAP isobath shifted landward over 300 m in the 17 months investigated. Simultaneously, the alongshore extent of the peninsula increased: the shoreline prograded by up to 200 m over a stretch of 480 m northward of the peninsula and 710 m southward, resulting in an increase in the alongshore extent of the Sand Engine from 2450 to 3640 m (~50% increase).

The planform analysis shows that shoreline progradation can be observed by ~1200 m in the adjacent coastal sections. This provides a first estimate of the area of positive influence, but cross profile sediment movements were however not taken into account in this analysis. To assess whether the shoreline movement can be taken as a good proxy for the area which shows accretion by the nourishment the alongshore distribution of sedimentation and erosion was computed, integrating the bed level changes per cross-shore profile to obtain sediment volume changes per meter alongshore. The profile integrated volume change (Fig. 9b) shows a larger spread of sediment than the shoreline (Fig. 9a), revealing that the shoreline motion underestimates the spreading of sediment slightly in this case. Fig. 9b also reveals accretion on both sides of the nourishment and the expansion over time. Especially on the northern side this is visible as the northern limit of the accreting profiles was shifting from $y \sim 2100$ m after 3 months to $y \sim 3000$ m after 17 months. By then, the accretional profiles extended over 4.5 km along the entire stretch of the surveyed domain. The most southern
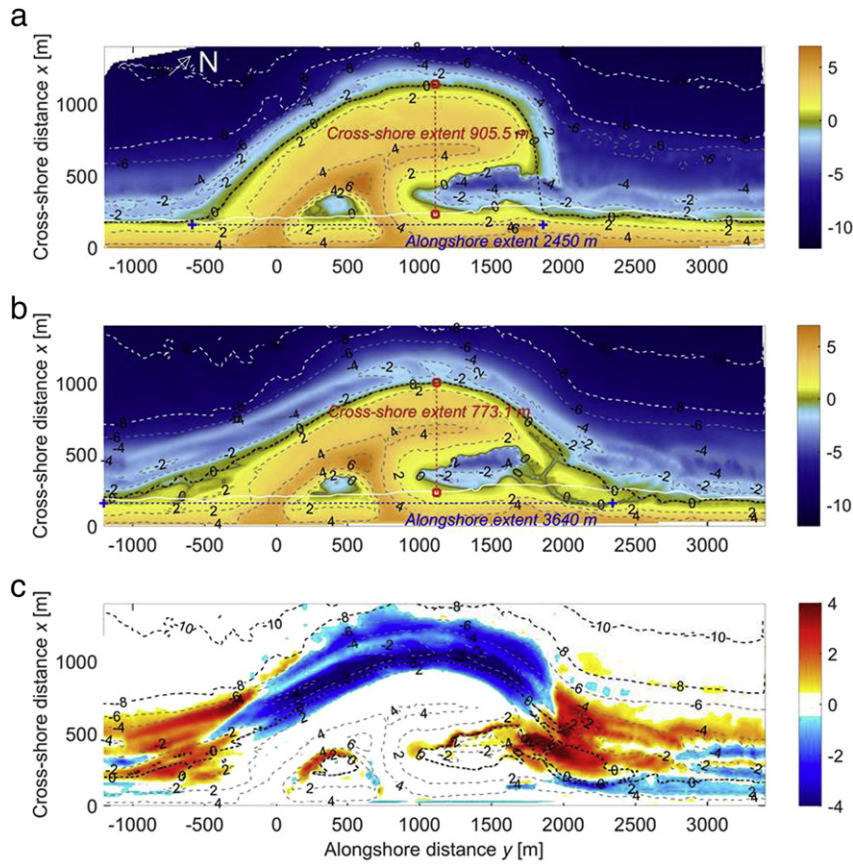
Fig. 8. Change in shape of the Sand Engine peninsula in the first 17 months. Panels a) and b) show the bed elevation in meters NAP for August 2011 (first survey) and December 2012 (last survey). The 0 m isobath as used for the planform shape analysis is given by the thick black dashed line. The 0 m isobath on the beach prior to the construction given by the solid white line. Panel c) shows the sedimentation (red colours) and erosion (blue) in meters based on the two surveys. Contour lines in panel c) are of the last survey, with the 0 m isobath highlighted by the thick dashed line.

profiles (near $y = -1300$ m) show substantial accretion at the border of the survey domain, indicating that the survey domain may not be fully encompassing the influence region of the Sand Engine. For future evaluation of the feeding beyond the edge of the survey domain an on-going monitoring campaign with less frequent surveys but increased alongshore scale was initiated (de Vries et al., 2014).
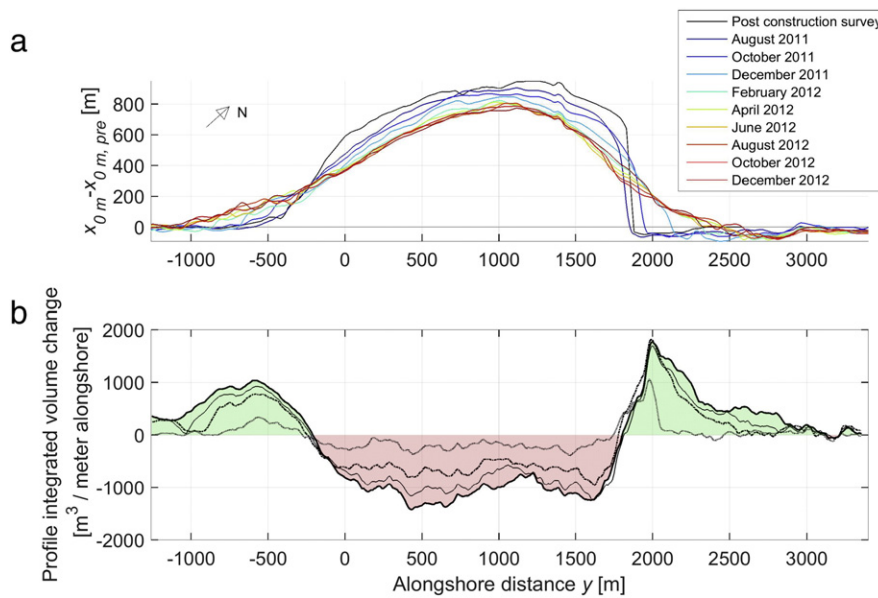

Fig. 9. a) Most seaward cross-shore position of the 0 m NAP contour with respect to its position prior to the nourishment. Coloured contour lines display a selection of the surveys, approximately two months apart. Black line corresponds to the 0 m contour in the post-construction survey by the contractor. b) Cumulative bed level changes integrated over the cross-shore profile with respect to the first survey. Dotted, dash-dotted, thin and thick solid lines represent the situation after 3, 6, 12 and 17 months respectively.
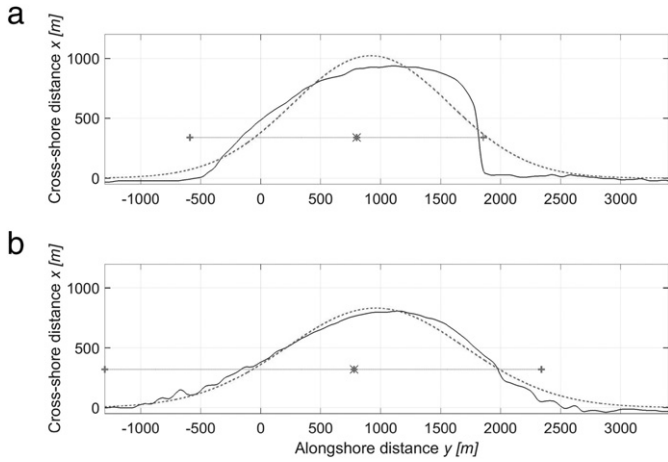
Fig. 10. Example 0 m NAP contours of the Sand Engine (solid lines) and the derived parameters for a) the first survey (August 2011) and b) the last survey (December 2012). The alongshore position of the centre of mass, m_1, of the planform shape is indicated with the * symbol. Both + signs indicate the alongshore position of crossing of the 0 m contour with the 0 m contour in the pre-construction survey. The dashed lines show the best fitted normal distributions $x_{0m}'(y)$ for each of the planform shapes.

The planform transformation was subsequently quantified for each survey using the following 5 parameters:

- The maximum cross-shore extent X_{max}, i.e. the maximum cross-shore distance of the 0 m NAP contour $x_{0m}(y)$ with respect to its position prior to construction $x_{0m,pre}(y)$ (see Fig. 8).
- The centre of the planform shape m_1, calculated as the first order central moment of $x_{0m}(y)$. The centre-point was used to examine advection of the nourishment shape (Fig. 10).

- The width of the peninsula, s_{left} and s_{right}, i.e. the spread to either side of the centre of mass as calculated by the distance on both sides between the centre-point m_1 and the crossings of the current 0 m contour $x_{0m}(y)$ with $x_{0m,pre}(y)$ (Fig. 10).
- The skewness of the outline $\gamma_y = m_3/m_2^{3/2}$, as calculated from the third and second order central moments of the imaginary part of the Hilbert transform of $x_{0m}(y)$. Parameter γ_y shows the asymmetry of the shape about the cross-shore axis and to what extent the outline was slanted in a particular direction.
- The similarity with a Gaussian bell shape function. A Gaussian function $x_{0m}'(y) = ae^{-\frac{1}{2}\left(\frac{y-y_p}{\sigma}\right)^2}$ was fitted, where parameters a and y_p define the cross-shore amplitude and alongshore location of the centre of the Gaussian hump and σ defines the spread of the shape. The three parameters were optimized using a least squares method on the difference between cross-shore location of the 0 m contour, $x_{0m}(y)$, and the fit, $x_{0m}'(y)$. The root mean squared error $RMSE$ between the fit and the contour indicates how well the contour resembles a Gaussian function.

As can be seen in Fig. 11a, the reduction in X_{max} was largest in the first half year and notably during January 2012, coinciding with the largest storm (see Fig. 7). The remainder of the data show a gradual decrease in X_{max} without large variations. The m_1 centre-point of the nourishment shape varied around alongshore position $y = 790$ m (standard deviation σ_{m_0} was < 20 m) with a small (20 m) southward migration over the time period considered. At the same time the spread to both sides (s_{left} and s_{right}) of the centre-point increased (Fig. 11 b), reflecting the increase in width. During the first year the alongshore width increased by about 90 m per month. No signature of energetic months can be observed. In contrast, the monthly increase in s_{left} and s_{right} was largest during the mild energetic months in spring 2012.

During the first 8 months the Sand Engine evolved from the man-made strongly asymmetric ($\gamma_y \sim 1$, Fig. 11c) shape to a near symmetrical
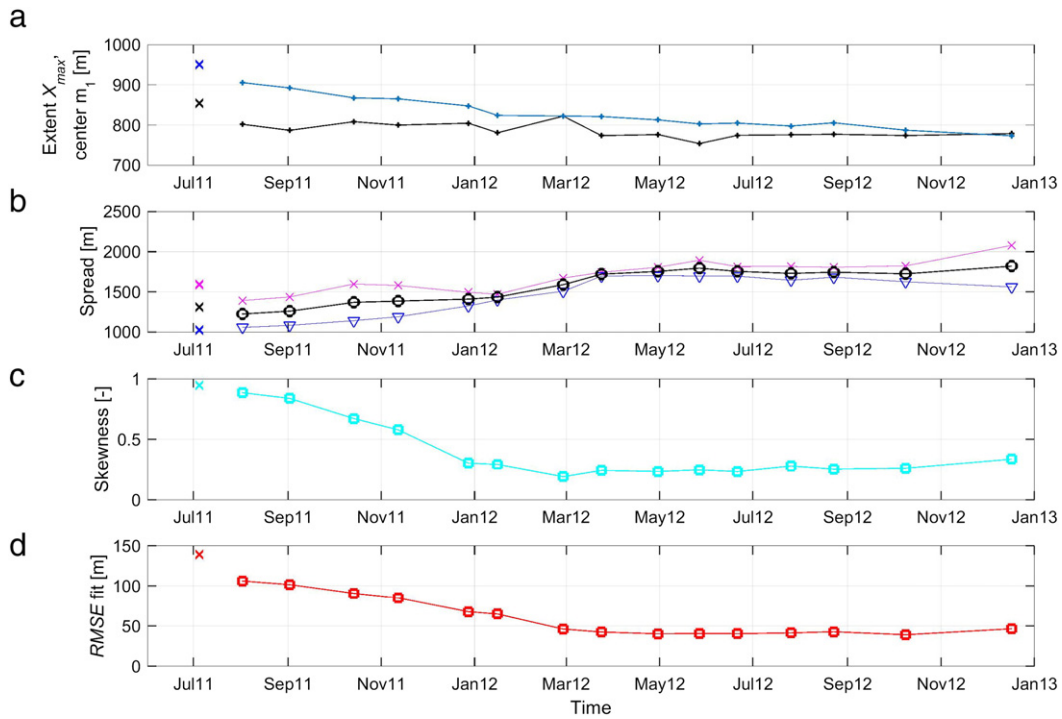

Fig. 11. Planform adjustment of the Sand Engine peninsula over time. a) The maximum cross-shore extend X_{max} (blue line) and the centre of mass of the planform shape m_1 (black line). b) Mean spread of the distribution (black line) and the spread to southern (northern) side s_{left} (s_{right}) of the centre of mass in magenta (blue). c) Skewness γ_y of the planform shape. Negative values indicate a skew towards the northeast. d) The root-mean-squared error $RMSE$ between the best-fitted Gaussian function and the measured contour. Cross symbols in July 2011 represent values as extracted from the post construction survey by the contractor.

shape ($\gamma_y \sim 0.2$). This also caused a substantial reduction in *RMSE* (Fig. 11d), implying the evolution into a Gaussian shape. After this first period γ_y remained ~ 0.2 and *RMSE* was about constant. The rapid shape resemblance to a Gaussian distribution function corresponds well to the conceptual picture of planform evolution and diffusion of a rectangular nourishment as originally presented by Pelnard-Considère (1956) (in: Dean, 2002).

To summarize, the data show that, despite its particular initial shape the Sand Engine peninsula quickly transformed to a diffusive form with a smooth shoreline, a rapid decrease in cross-shore extent and a large alongshore increase in width to both sides. The timescale of the adjustment was about a year, after which changes to the shape became less pronounced.

4.3. Quantification of the feeding of adjacent coasts

The overall ratio of the feeding behaviour was quantified using volume budgets of the peninsula and the adjacent sections. To that end, the survey domain was separated into 4 different surface areas (Fig. 12, insert): 1) the peninsula only, 2) the adjacent coast on the northern side, 3) the adjacent coast on the southern side and 4) the sum of changes in all three areas combined showing the net loss/gain in the total survey domain. The surface areas for volume calculations have a landward edge at the dune foot and were trimmed seaward at about the −10 m NAP, as here the bed level changes were small (see Fig. 8).

Over the 17 months we observe a loss of 1.8 10⁶ m³ on the peninsula alone (Fig. 12, red line), amounting to 11% of the 16 10⁶ m³ of added volume during the construction in this area. The majority of the erosion took place during the first 6 months, and especially during December 2011 and January 2012. For a more traditional evaluation of a nourishment, the remaining volume in this area would be a measure for the success of the project (e.g. Dean, 2002; Dean and Yoo, 1992; Elko and Wang, 2007; Verhagen, 1996). However as the Sand Engine nourishment was intended to feed the adjacent coasts it was essential to combine the loss with the accretion volumes in the adjacent coastal sections. Both adjacent coastal sections show accretion (Fig. 12, blue and magenta lines) although a slightly larger volume was found in the northern section. This is in line with existing knowledge on net northward sediment transport on this part of the coast (e.g. van Rijn, 1997); however, it must also be noted that the accretion on the southern side was likely to extend beyond the southern border of the measurement domain (see Fig. 9 b). Therefore, the accretion to the south of the peninsula might be underestimated. In total, an increase in sediment volume of 1.3 10⁶ m³ was found at both sides combined. This implies that losses on the peninsula were for a large part (72%) compensated for by accretion the adjacent coastal sections.

Overall, the surveyed area experiences a loss of sand of 0.5 10⁶ m³, a loss which was primarily growing during the energetic winter months. These losses could be attributed to the southern boundary being very close to the peninsula and the accretion observed at this boundary. Furthermore these losses can be due to consolidation of the subsoil,
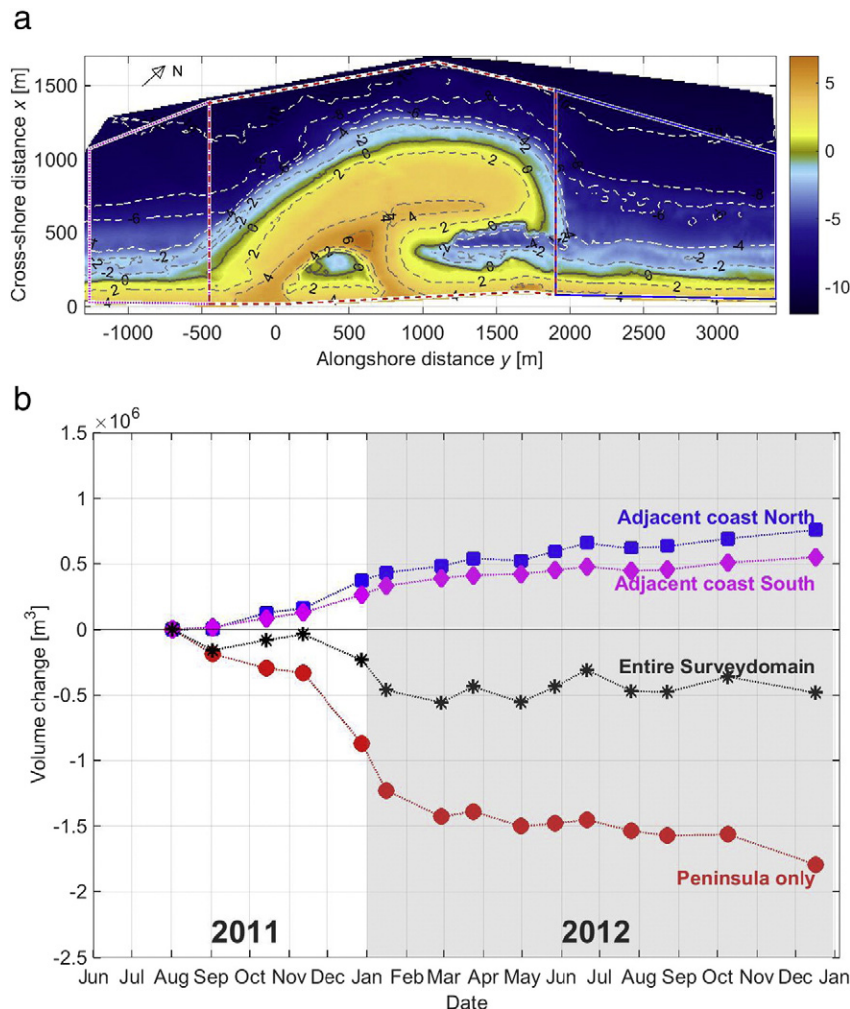

Fig. 12. a) Surface areas used for the sediment budgets. b) Cumulative volumetric changes of the Sand Engine peninsula (in red) and the adjacent coastal sections north (blue) and south (magenta) with respect to the first survey of August 2011. Black symbols indicate the volume change in the three zones combined.

washing out of fines, transport towards the dunes, transports to off-shore (< − 10 m NAP) or more northward. To examine the feeding towards the dunes, the Lidar surveys were analysed. A small foredune area was selected landward of the areas used for the volume budgets on beach and shore face in Fig. 12. This foredune area with the first dune row captures the region around the dune face between approximately + 4 and + 10 m NAP and was on average 50 m wide in the cross-shore direction. The biannual Lidar surveys were not executed simultaneously with other surveys but provide data on the bed elevation in the dunes every 6 months. The increase in volume in the dune area was about 0.1 10^6 m^3 in the first 18 months, i.e. ~15 m^3 per m alongshore per year. This magnitude corresponds well to values reported by (van der Wal, 2004) (14 m^3/m/year) for nourished beaches and de Vries et al. (2012) (0–40 m^3/m/year) at the Dutch coast. Thus at least 20% of the losses in the survey domain can be attributed to eolian transport towards the dunes.

4.4. Changes in feeding on a monthly timescale

The previous two sections examined the overall redistribution of sand to adjacent coastal sections in terms of changes in shape and volume of the peninsula. The main objective of this section is to analyse the variations in the redistribution on a monthly timescale, as the time series of the volume change of the peninsula revealed that the erosion volumes varied from one survey period to another (Fig. 12, red line).

4.4.1. Changes in the spatial pattern of the redistribution of sediment on a monthly timescale

Plan view images of the bed level changes in between consecutive surveys (Fig. 13) show that not only the magnitude but also the alongshore patterns in bed level change varied with time. For a time period with energetic (oblique) wave action, as found during autumn and winter, the sedimentation and accretion varied along the perimeter (Fig. 13a). The convex tip of the Sand Engine eroded while the adjacent concave coastline sections predominantly accreted. These conditions therefore resulted in a smoothing of the outline and feeding from the nourishment to adjacent coasts. The pattern of erosion along the convex coastline and sedimentation along the concave adjacent sections confirms the schematic example of sediment redistribution of nourishments under small-angle waves (e.g. Dean, 2002; Elko and Wang, 2007). Contrary to the period with energetic wave action, the changes during a month with mild wave action were nearly uniform along the perimeter of the peninsula (Fig. 13b). For the specific time period with mild wave action shown here, the sedimentation erosion pattern bears resemblance to the cross-shore generation of a summer berm (e.g. Inman et al., 1993; Quartel et al., 2008), with sedimentation just above mean sea level and erosion below mean sea level.

The examples in Fig. 13 suggest a relation between wave conditions and the patterns in feeding, but the level of dependency cannot be quantified easily as the observed differences from one survey to another do not solely originate from the environmental conditions. More generally the controls for the changes to the feeding on a monthly timescale can be subdivided into three categories: 1. the environmental conditions (e.g. wave height), where more energetic wave conditions yield larger gradients in transport (e.g. Splinter et al., 2010); 2. the cross-shore profile (e.g. cross-shore slope of the surf zone), where steeper slopes yield larger transports (Kamphuis, 1991; Mil-Homens et al., 2013) and 3. the planform shape (e.g. shoreline curvature), where strongly curved coasts experience more lateral dispersion (Dean, 2002; Dean and Dalrymple, 2002). During the first period after construction of a nourishment none of these categories were likely to be invariant and therefore we examined parameters of the three categories side-by-side.

4.4.2. Cross-shore profile adjustments

First, the cross-shore profile changes are shown in detail to show the adaptation of the man-made profile to a more natural profile for a transect south (Fig. 14 a), in the centre (Fig. 14 b) and north of the peninsula (Fig. 14 c). The adjacent coast south of the Sand Engine peninsula was subject to a large (1000 m^3/m) increase in sediment (Fig. 9 b). The majority of the sand was deposited in the surf zone and upper shoreface between 0 and − 6 m NAP, indicative of the active zone on this timescale. Beyond − 6 m, the bed level changes were small. Rapidly after construction a subtidal bar formed, which growed vertically in the first months and then moved slightly downslope (Fig. 14a; yellow and green lines near x = 500 m). In the 18 months investigated here no signature was present of cyclic bar behaviour as found on other parts of the Dutch coast. However, as typical timescales of cyclic bar behaviour is 4–16 years (Ruessink et al., 2003), this has to be evaluated after further continuation of the monitoring. In the supra-tidal profile small variations can be observed (<0.2 m above the 3 m NAP contour), but overall the upper beach hardly changed.

Towards the centre of the Sand Engine the profile primarily eroded (Fig. 14b). The steep convex profile implemented by the contractor (black line) adjusted to a concave erosional profile, with the slope the profile reducing quickly, i.e. from 1:32 to 1:45 in the first 5 months for the zone + 1 m to − 4 m. After 18 months the mean sea level isobath retreated by about 150 m and the profile slope was 1:53, similar to the natural slope of 1:55 prior to the nourishments. The reshaped profile mimicked a compound double concave profile with the top concave part of the profile running from the berm top (+ 3 m NAP) to mid-surf zone (− 2.5 m NAP) and a second continuous concave slope downward from − 2.5 m NAP. As a result the overall average slope in the zone + 1 m to − 6 m NAP reduced greatly, yet the part around and above mean sea level remained very steep (<1:20). A similar adjustment of the profile was previously reported at other nourishments (e.g. at Hunting Island, USA; Kana and Mohan, 1998).

North of the Sand Engine peninsula the profiles were influenced by the formation of the spit and the tidal channel connecting the lagoon (Fig. 14c). Similar to the profiles south of the peninsula, a subtidal bar formed. The seaward slope of the bar matched the slope of the shoreface nourishment executed in this coastal stretch. Higher up the profile a large intertidal bar with a cross-shore width of more than 200 m formed because of the spit feature. This bar migrated slowly landwards (50 m in the last 12 months) and forced the channel into the supra-tidal beach, similar to the observations of channel movement by Cheung et al. (2007) at a natural spit.

All profiles show the formation of a smooth compound concave up profile with a tipping point at the subtidal bar crest (at app. -3 m NAP). Such a compound profile is comparable to previous observations at ocean beaches (Inman et al., 1993). For the Dutch coast without groynes however, it is more common to find multiple barred beaches (Ruessink and Kroon, 1994; Wijnberg and Terwindt, 1995). Whether a multiple bar will eventually form, can be assessed only from the continuation of our monitoring on longer timescales.

4.4.3. Ratio of along- and cross-shore adjustment

The cross-shore sediment motions coincide with the planform changes. In an attempt to divide the cross and alongshore adaptations, the gross and the net bed level changes within a profile were calculated per alongshore location from consecutive surveys (see Fig. 15a):

$$\Delta V_{p,gross}(y) = \sum_x |z_i(x,y) - z_{i-1}(x,y)| \Delta x, \qquad (1)$$

$$\Delta V_{p,net}(y) = \left| \sum_x z_i(x,y) - z_{i-1}(x,y) \Delta x \right|, \qquad (2)$$

where $z_i(x,y)$ was the transect data and index i indicates the survey number. $\Delta x = 10$ m was the cross-shore spacing of the interpolated
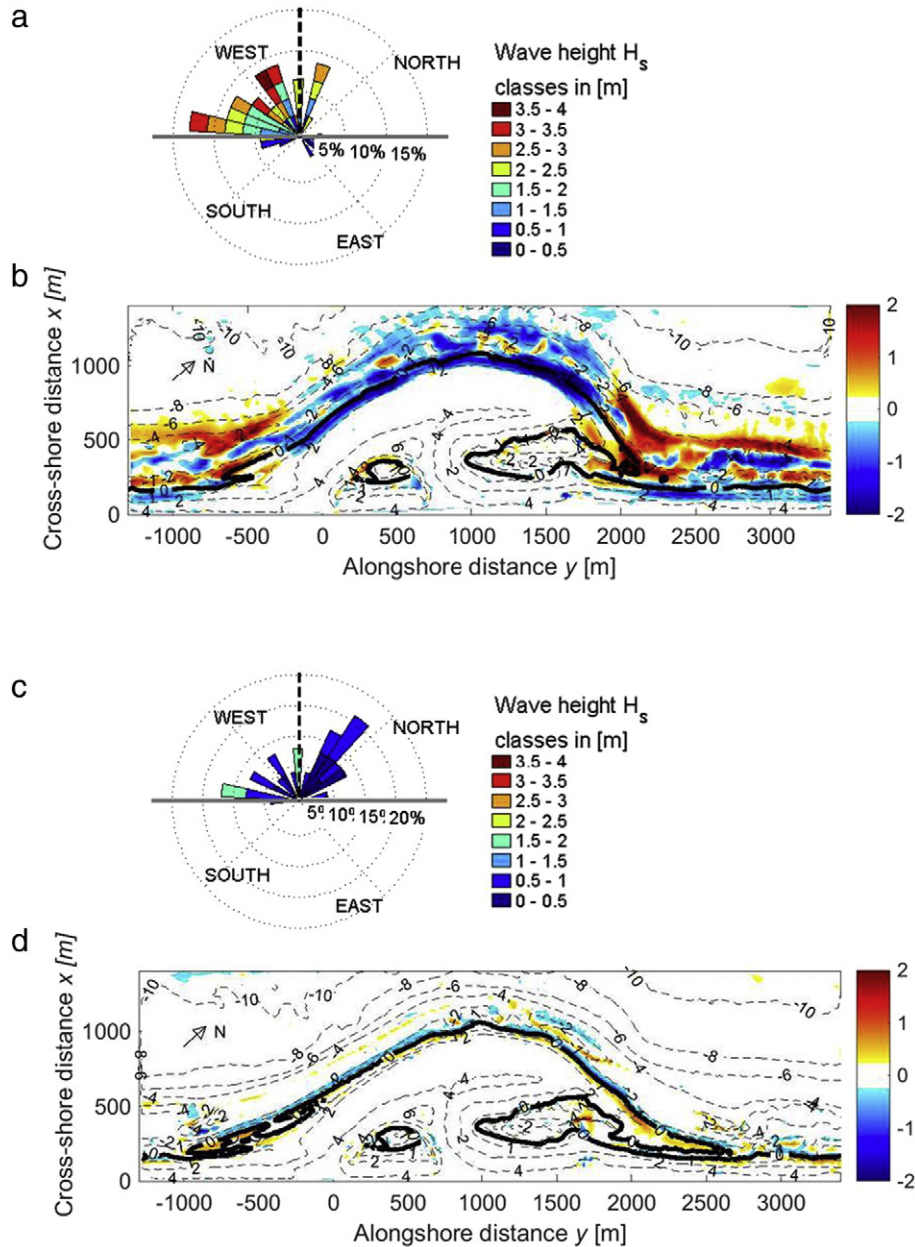
Fig. 13. Sedimentation and erosion patterns and concurrent wave conditions on a monthly timescale for an energetic period (mid-November and end of December 2011) and a mild wave period (end of February and mid-March 2012). Wave roses show the wave climate as measured offshore between consecutive surveys for a) energetic and c) mild wave conditions and were rotated to align with the shoreline orientation. Panels a) and b) show the wave conditions and bed level change in meters between mid-November and end of December 2011. Panels c) and d) show the wave conditions and bed level change in meters between end of February and mid-March 2012. Contour lines in panels b) and d) show the bed elevation of December 2011 and March 2012 respectively, with the 0 m NAP isobath highlighted by the thick dashed line.

transect data. The ratio of both values, $R(y) = \Delta V_{p,net}(y)/\Delta V_{p,gross}(y)$, was used to indicate to what extent the bottom changes were related to alongshore feeding. If the ratio $R(y)$ equaled unity, i.e. net and gross volume changes were equal, erosion or accretion can be thought of as predominantly alongshore. In contrast, if the ratio $R(y)$ equaled zero then volume loss in profiles due to erosion was fully compensated for by accretion as would be the case by a purely cross-shore displacement of sediment. The volume changes $\Delta V_{p,net}(y)$, $\Delta V_{p,gross}(y)$ and ratio R were alongshore integrated over the zone $-250 < y < 1750$ m, which is the eroding outer perimeter of the peninsula.

The results displayed in Fig. 16a show that the net volume change between consecutive surveys varied widely over the investigated period from ~1300 m^3 to ~550.000 m^3. Especially the first months showed

large volume changes, while for some months in early 2012 hardly any net change was observed. Gross changes show far less variation (from ~160.000 m^3 to ~770.000 m^3, i.e. a factor 5) yet still substantial gross volume changes took place within the profile. R values varied between survey periods (Fig. 16b), with the temporal fluctuation highlighting the difference in feeding behaviour in these months.

4.4.4. Potential controls on the spreading of sediment

The alongshore averaged parameters for the gross and net volume changes (ΔV_{gross}, ΔV_{net}) on the tip of the Sand Engine ($-250 < y < 1750$ m) were compared to three potential controls to examine their influence on the magnitude of the feeding and the observed variation in
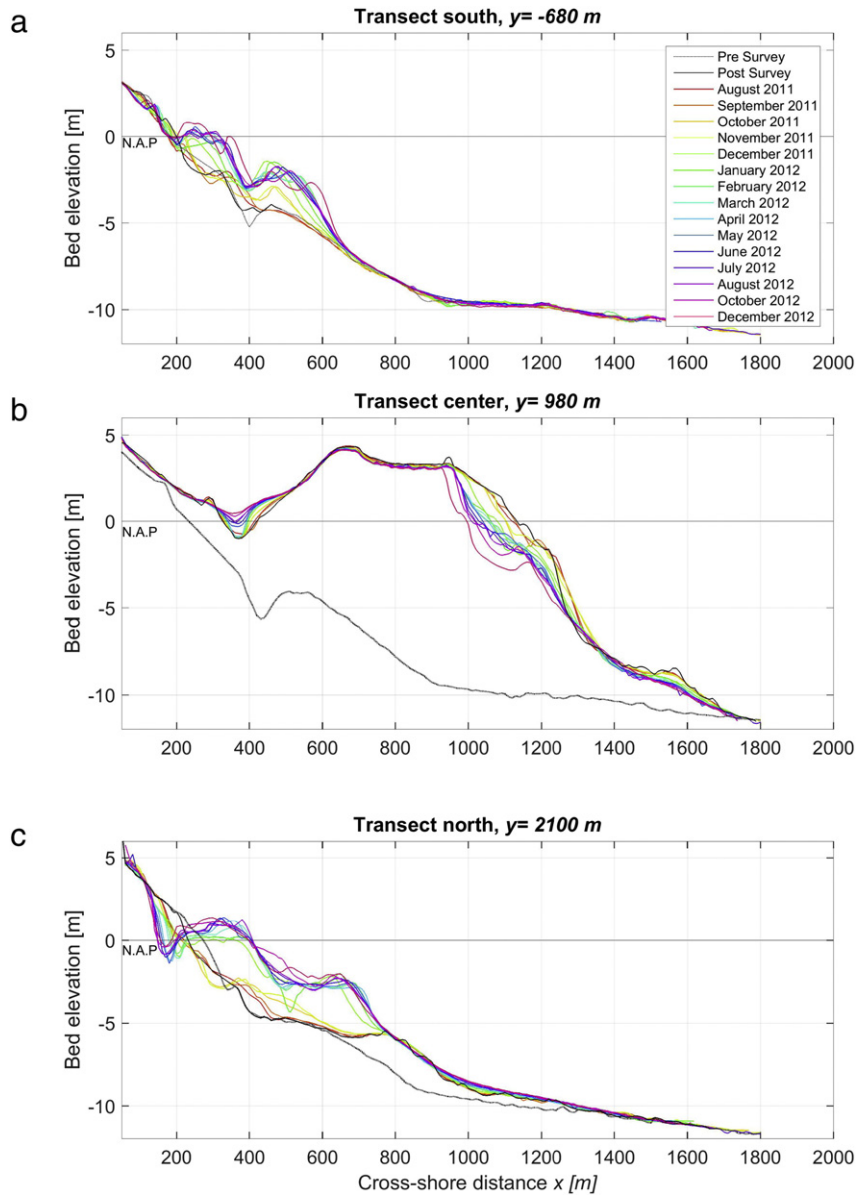
Fig. 14. Cross-shore transects a) south of the peninsula, b) near the centre and c) north of the peninsula. Coloured lines show the different surveys; pre- and post construction surveys by the contractor are given by the black dashed and solid lines, respectively.

volume change of the peninsula on a monthly timescale. The selected parameters were proxies for:

1. <u>Wave forcing</u> magnitude. The average offshore wave power $\overline{P_0} = 1/16\rho g H_s^2 c_g$ and the cumulative wave power $P_{0,cum} = \sum 1/16\rho g H_s^2 c_g$ between consecutive surveys were used as proxies, with ρ being

the specific density of seawater in [kg/m^3], g the gravitational acceleration in [m/s^2]and c_g the wave group velocity in [m/s] determined using linear wave theory and the measured wave period.

2. The cross-shore profile. We examined if an effect of the slope of the cross-shore profile on alongshore transport could be distinguished,
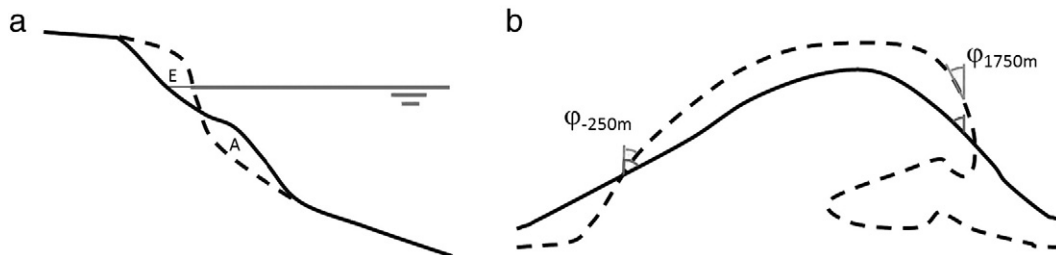

Fig. 15. a) Schematic to illustrate the difference between the gross volume changes $\Delta V_{p,gross}$ (areas A + E) and net volume changes $\Delta V_{p,net}$ (A–E) in a profile, b) Method used to define the difference in coastline angles.
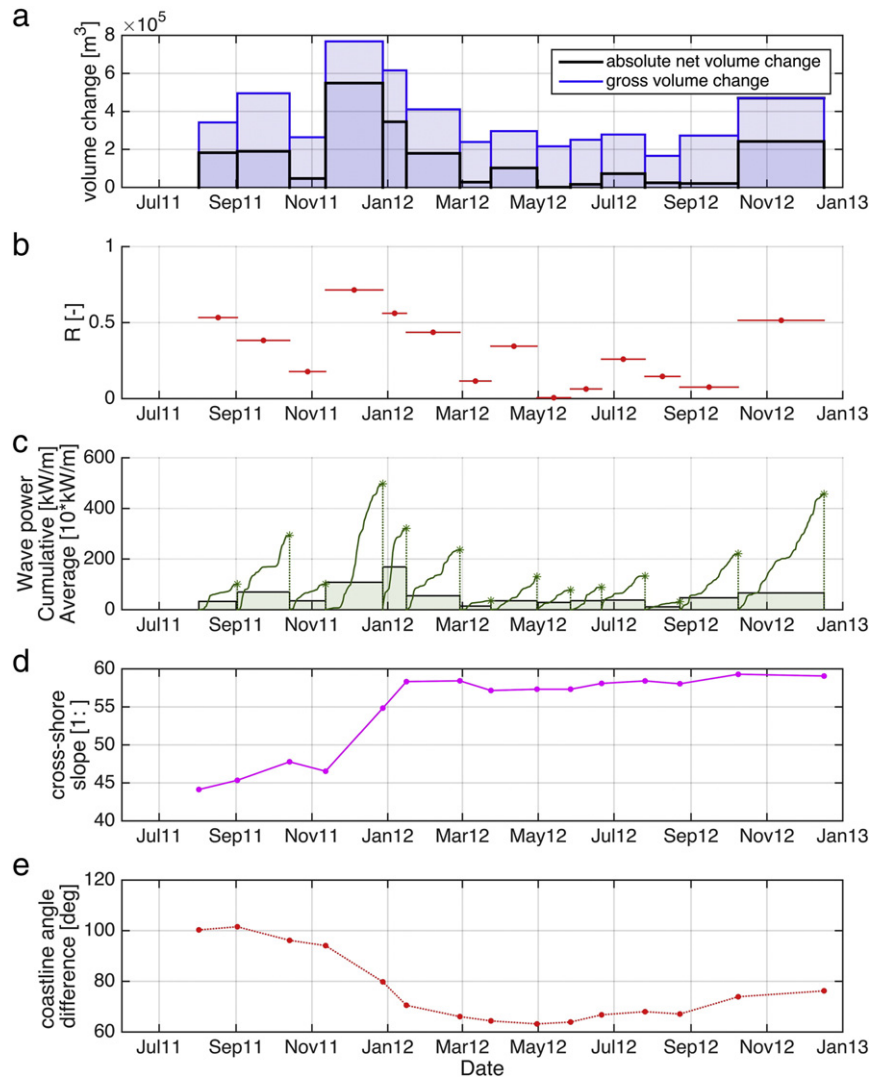
Fig. 16. Changes at the Sand Engine peninsula on a monthly timescale (i.e. per survey period). Panels show a) the volume changes on the tip of the Sand Engine, b) the ratio R of volume displacements within the profiles vs. the volume losses out of the profiles, c) cumulative and average wave power offshore between two surveys, d) cross-shore slope between the $+1$ and -4 m NAP and e) the difference in coastline angle between the two edges of the peninsula. Values in panels a), b) and d) are the average values for the outer edge of the peninsula ($-250 < y < 1750$ m).

as suggested by Kamphuis (1991) and Mil-Homens et al. (2013). Since the long term development of the Sand Engine was estimated to be dominated by waves of about 2.5 m (Kaji et al., 2014), the average slope of the surf zone dz_{sz}/dx in the zone $+1$ an -4 m NAP was used as slope to be evaluated.

3. The planform shape. The coastline angles on both sides of the peninsula were compared (Fig. 15b) to test for a dependency of the amount of curvature in the coastline to the lateral dispersion, such that stronger curved coasts yield to large gradients in alongshore sediment transport and therefore stronger losses (Dean and Dalrymple, 2002; Elko and Wang, 2007; Komar, 1998). The difference in coastline orientation $\Delta\varphi$ was computed between $y = -250$ m and $y = 1750$ m, spatially coinciding with the transition point between the erosional outer convex shoreline and the adjacent sedimentation (see Fig. 9b) and similar to the coastal stretch used to compute volume changes.

The parameters were extracted for each survey period and are displayed in Fig. 16c, d and e. Relationships between the volumetric feeding parameters (ΔV_{net}, ΔV_{gross}, R) and the potential controls were quantified using least squares linear regression, with the resulting correlation coefficients between individual pairs given in Table 1.

Across a range of parameters examined the strongest relation with the volumetric losses was found for the offshore wave forcing. Wave power varied over the survey periods, showing a signature of the seasonality in the wave forcing with large mean wave power ($\sim 2 10^4$ kW/m) during fall and winter periods, while spring months coincided with far less wave power ($\sim 1 10^3$ kW/m). The time series of the ΔV_{net} (Fig. 16a, black boxes) showed a strong significant correlation with both the cumulative $P_{0,cum}$ ($r = 0.85$, i.e. $r^2 = 0.72$) and the average $\overline{P_0}$ ($r = 0.79$) wave power per survey period. This quantifies the observation that months with strong wave forcing coincided with large erosion on the tip. As the morphological changes were limited during the months with relatively low incoming wave power it can be concluded

Table 1
Correlation coefficients r of influencing parameters on the volume changes on the peninsula on a monthly timescale. Values that were not significant to the 95% confidence interval were striked through.

	ΔV_{net}	ΔV_{gross}	R
Average wave power $\overline{P_0}$	0.79	0.86	0.68
Cumulative wave power $P_{0,cum}$	0.85	0.90	0.76
The average surf zone slope dz_{sz}/dx	~~-0.10~~	~~-0.09~~	~~-0.21~~
Coastline curvature $\Delta\varphi$	~~0.26~~	~~0.27~~	~~0.37~~

that the motion of the horizontal tide, which can be of 0.5–1 m/s in this region, was by itself insufficiently large to generate the feeding behaviour to adjacent coasts. This confirms earlier findings of the limited effect of tidal motion on nourishment behaviour by Grunnet et al. (2005) based on numerical model simulations. The strong positive correlation of R with the wave forcing ($r = 0.68$) supports the observation that with mild wave action mostly cross-shore changes occurred, with relatively minor net volume loss on the tip and consequently no feeding of the adjacent coasts.

A large change in cross-shore profile slope was observed, with the average slope over the outer edge decreasing from 1:44 to 1:58. The slope adjustment took place in a episodic manner coinciding with the energetic winter period. This temporal behaviour provided no correlation with the observed volume changes on the timescale of months. Similar findings were found for the coastline angle difference. The difference between these coastline angles at either side of the peninsula was large (~100°) in the first surveys. Over time the shape became smoother and the coastline difference angles reduced to 65–75° (Fig. 16e). Although the curvature of the planform shape plays an important role for the erosional volumes in the conceptual view of dispersion of blunt nourishments shapes (e.g. Elko and Wang, 2007), this was not reflected in a significant correlation for the first 18 months of the Sand Engine evolution.

The relatively static behaviour of the cross-shore slope and coastline curvature in the 17 months and the large dependence of volume changes on the wave power obscures a correlation between the secondary effects i.e. the effect of the slope and curvature on erosional volumes. A partial correlation analysis for three variables was performed to test the dependency of volume changes on the wave power was computed while controlling for the profile slope (or coastline angle). The partial correlation analysis confirmed the dependency of volume losses on wave power but did not improve the correlations nor reveal a significant effect of the profile slope (coastline curvature) due to the small correlation between the wave power and the profile slope (coastline curvature). It was however noticed that the first two periods after construction (with steep slopes and strong curvature) experienced more erosion than other months with similar wave forcing (Fig. 16a).

Summarizing, the data reveal that the differences in feeding behaviour on a monthly timescale were primarily connected to the magnitude of the wave forcing. An effect of the morphology (planform curvature and cross-shore slope) might be present, but cannot be substantiated with this dataset.

5. Conclusions

Mega-scale nourishments feeding larger sections of coasts have been proposed as an alternative for regular nourishments to increase beach width and coastal safety. This paper presents the analysis of the morphological evolution of a 17 million m³ mega nourishment during the first 18 months after implementation. The observations show a planform adjustment of the mean-sea-level contour on the timescale of months as the original asymmetric outline was reworked to a nearly symmetrical shape. Along the outer perimeter of the peninsula the shoreline retreated O (150 m) in these 18 months, with some locations showing a retreat up to 300 m. Simultaneously, the shoreline prograded by up to 200 m in the adjacent coastal sections, resulting in an increase of the alongshore extent of 1200 m (50% increase). Within the measured 18 months after implementation the profile steepness in the region $+1$ to -4 m around mean sea level adjusted from a steep (~1:45) man-made slope to a 1:55 to 1:60 slope, which is similar to the natural slope steepness in this region, thus highlighting the different timescales of the cross-shore and alongshore adjustments. The surveys show that the volumetric losses on the nourished peninsula were 1.8×10^6 m³, i.e. about 10% of the added volume. The majority (70%) of the volumetric losses in sediment on the peninsula were found to be compensated by accretion on adjacent coastal sections and dunes,

confirming the feeding property of the nourishment. Further analysis shows that the morphological response was strongest in the first 6 months while the planform curvature and the surf zone slope reduced. In the following 12 months changes were less pronounced. Overall, the feeding property was related to incident wave power, such that months with high-energy waves result in more alongshore spreading. Months with small wave heights resulted mostly in cross-shore movement of the nourished sediment.

References

Ashley, G.M., 1990. Classification of large-scale subaqueous bedforms: a new look at an old problem bedforms and bedding structures. J. Sediment. Res. 60 (1), 160–172.

Burcharth, H.F., et al., 2015. Chapter 3 — innovative engineering solutions and best practices to mitigate coastal risk. In: Zanuttigh, B., Nicholls, R., Vanderlinden, J.P., Burcharth, H.F., Thompson, R.C. (Eds.), Coastal Risk Management in a Changing Climate. Butterworth-Heinemann, Boston, pp. 55–170.

Castelle, B., Turner, I.L., Bertin, X., Tomlinson, R., 2009. Beach nourishments at Coolangatta Bay over the period 1987–2005: impacts and lessons. Coast. Eng. 56 (9), 940–950.

Cheung, K.F., Gerritsen, F., Cleveringa, J., 2007. Morphodynamics and sand bypassing at Ameland inlet, the Netherlands. J. Coast. Res. 106–118.

Cooke, B., Jones, A., Goodwin, I., Bishop, M., 2012. Nourishment practices on Australian sandy beaches: a review. J. Environ. Manag. 113, 319–327.

de Vries, S., Southgate, H., Kanning, W., Ranasinghe, R., 2012. Dune behavior and aeolian transport on decadal timescales. Coast. Eng. 67, 41–53.

de Vries, S., de Schipper, M.A., Stive, M.J.F., 2014. Measured gradients in alongshore sediment transport along the Dutch coast. Proc. Int. Conf. Coast. Eng. 1 (34), 43–58.

Dean, R.G., 2002. Beach nourishment: theory and practice vol. 18. World Scientific Press (399 pp.).

Dean, R.G., Dalrymple, R.A., 2002. Coastal Processes with Engineering Applications. Cambridge University Press.

Dean, R.G., Yoo, C.H., 1992. Beach-nourishment performance predictions. J. Waterw. Port Coast. Ocean Eng. 118 (6), 567–586.

Elko, N.A., Wang, P., 2007. Immediate profile and planform evolution of a beach nourishment project with hurricane influences. Coast. Eng. 54 (1), 49–66.

FitzGerald, D.M., 1982. Sediment bypassing at mixed energy tidal inlets. Proc. Int. Conf. Coast. Eng. 1 (18), 1094–1118.

Grunnet, N.M., Ruessink, B.G., 2005. Morphodynamic response of nearshore bars to a shoreface nourishment. Coast. Eng. 52 (2), 119–137.

Grunnet, N.M., Ruessink, B.G., Walstra, D.J.R., 2005. The influence of tides, wind and waves on the redistribution of nourished sediment at Terschelling, the Netherlands. Coast. Eng. 52 (7), 617–631.

Hamm, L., Capobianco, M., Dette, H.H., Lechuga, A., Spanhoff, R., Stive, M.J.F., 2002. A summary of European experience with shore nourishment. Coast. Eng. 47 (2), 237–264.

Hanson, H., Brampton, A., Capobianco, M., Dette, H., Hamm, L., Laustrup, C., Lechuga, A., Spanhoff, R., 2002. Beach nourishment projects, practices, and objectives: a European overview. Coast. Eng. 47 (2), 81–111.

Hoekstra, P., Houwman, K.T., Kroon, A., Ruessink, B.G., Roelvink, J.A., Spanhoff, R., 1996. Morphological development of the Terschelling shoreface nourishment in response to hydrodynamic and sediment transport processes. Proc. Int. Conf. Coast. Eng. 1 (25), 2897–2910.

Huang, J., Jackson, D.W., Cooper, J.A.G., 2002. Morphological monitoring of a high energy beach system using GPS and total station techniques, Runkerry, Co. Antrim, Northern Ireland. J. Coast. Res. 36 (36), 390–398.

Inman, D.L., Elwany, M.H.S., Jenkins, S.A., 1993. Shorerise and bar-berm profiles on ocean beaches. J. Geophys. Res. 98 (C10), 18,181–18,199.

Janssen, G., Kleef, H., Mulder, S., Tydeman, P., 2008. Pilot assessment of depth related distribution of macrofauna in surf zone along the Dutch coast and its implications for coastal management. Mar. Ecol. 29, 186–194.

Kaji, A.O., Luijendijk, A.P., Van Thiel de Vries, J.S.M., de Schipper, M.A., Stive, M.J.F., 2014. Effect of different forcing processes on the longshore sediment transport at the Sand Motor, the Netherlands. Proc. Int. Conf. Coast. Eng. 1 (34), 71–82.

Kamphuis, J., 1991. Alongshore sediment transport rate. J. Waterw. Port Coast. Ocean Eng. 117 (6), 624–640.

Kana, T.W., Mohan, R.K., 1998. Analysis of nourished profile stability following the fifth Hunting Island (SC) beach nourishment project. Coast. Eng. 33 (2–3), 117–136.

Komar, P.D., 1998. Beach processes and sedimentation. Prentice Hall (429 pp.).

Kuang, C., Pan, Y., Zhang, Y., Liu, S., Yang, Y., Zhang, J., Dong, P., 2011. Performance evaluation of a beach nourishment project at West Beach in Beidaihe, China. J. Coast. Res. 769–783.

Leonard, L., Clayton, T., Pilkey, O., 1990. An analysis of replenished beach design parameters on US East Coast barrier islands. J. Coast. Res. 15–36.

Luo, S., Cai, F., Liu, H., Lei, G., Qi, H., Su, X., 2015. Adaptive measures adopted for risk reduction of coastal erosion in the People's Republic of China. Ocean Coast. Manag. 103, 134–145.

Mil-Homens, J., Ranasinghe, R., van Thiel de Vries, J.S.M., Stive, M.J.F., 2013. Re-evaluation and improvement of three commonly used bulk longshore sediment transport formulas. Coast. Eng. 75, 29–39.

Mulder, J.P.M., van de Kreeke, J., van Vessem, P., 1994. Experimental shoreface nourishment, Terschelling (the Netherlands). Proc. Int. Conf. Coast. Eng. 1 (24), 2886–2899.

Niemeyer, H.D., Kaiser, R., Knaack, H., 1996. Effectiveness of a combined beach and shoreface nourishment on the island of Norderney, East Frisia, Germany. Proc. Int. Conf. Coast. Eng. 1 (25), 4621–4634.

Ojeda, E., Ruessink, B.G., Guillen, J., 2008. Morphodynamic response of a two-barred beach to a shoreface nourishment. Coast. Eng. 55 (12), 1185–1196.

Pelnard-Considère, R., 1956. Essai de théorie de l'évolution des formes de rivage des plages de sable et de galets. IV'eme Journees de l'Hydraulique, Les Energies de la Mer, Question III, rapport 1, 74-1-10.

Peterson, C.H., Bishop, M.J., 2005. Assessing the environmental impacts of beach nourishment. Bioscience 55 (10), 887–896.

Quartel, S., Kroon, A., Ruessink, B.G., 2008. Seasonal accretion and erosion patterns of a microtidal sandy beach. Mar. Geol. 250 (1–2), 19–33.

Roberts, T.M., Wang, P., 2012. Four-year performance and associated controlling factors of several beach nourishment projects along three adjacent barrier islands, West-Central Florida, USA. Coast. Eng. 70, 21–39.

Ruessink, B.G., Kroon, A., 1994. The behaviour of a multiple bar system in the nearshore zone of Terschelling, the Netherlands: 1965–1993. Mar. Geol. 121 (3–4), 187–197.

Ruessink, B.G., Wijnberg, K.M., Holman, R.A., Kuriyama, Y., Van Enckevort, I.M.J., 2003. Intersite comparison of interannual nearshore bar behavior. J. Geophys. Res. 108 (C8), 3249–3261.

Ruggiero, P., Walstra, D.J.R., Gelfenbaum, G., van Ormondt, M., 2009. Seasonal-scale nearshore morphological evolution: field observations and numerical modeling. Coast. Eng. 56 (11), 1153–1172.

Speybroeck, J., et al., 2006. Beach nourishment: an ecologically sound coastal defence alternative? A review. Aquat. Conserv. Mar. Freshwat. Ecosyst. 16 (4), 419–435.

Splinter, K.D., Golshani, A., Stuart, G., Tomlinson, R., 2010. Spatial and temporal variability of longshore transport along the Gold Coast, Australia. Proc. Int. Conf. Coast. Eng. 1 (32), 2156–2167.

Stive, M.J.F., et al., 2013. A new alternative to saving our beaches from sea-level rise: the Sand Engine. J. Coast. Res. 29 (5), 1001–1008.

Valverde, H.R., Trembanis, A.C., Pilkey, O.H., 1999. Summary of beach nourishment episodes on the US East Coast barrier islands. J. Coast. Res. 1100–1118.

van der Wal, D., 2004. Beach–dune interactions in nourishment areas along the Dutch coast. J. Coast. Res. 317–325.

van Duin, M.J.P., Wiersma, N.R., Walstra, D.J.R., Van Rijn, L.C., Stive, M.J.F., 2004. Nourishing the shoreface: observations and hindcasting of the Egmond case, the Netherlands. Coast. Eng. 51 (8), 813–837.

van Koningsveld, M., Mulder, J.P.M., 2004. Sustainable coastal policy developments in the Netherlands. A systematic approach revealed. J. Coast. Res. 20 (2), 375–385.

van Rijn, L.C., 1997. Sediment transport and budget of the central coastal zone of Holland. Coast. Eng. 32 (1), 61–90.

van Rijn, L.C., et al., 1995. Sand budget and coastline changes of the central coast of Holland between Den Helder and Hoek van Holland in the period 1964–2040. Delft Hydraulics Report H2129.

van Son, S., Lindenbergh, R.C., De Schipper, M.A., De Vries, S., Duijnmayer, K., 2010. Monitoring bathymetric changes at storm scale. PositionIT, Nov/Decpp. 59–65.

Verhagen, H.J., 1996. Analysis of beach nourishment schemes. J. Coast. Res. 179–185.

Wijnberg, K.M., 2002. Environmental controls on decadal morphologic behaviour of the Holland coast. Mar. Geol. 189 (3), 227–247.

Wijnberg, K.M., Terwindt, J., 1995. Extracting decadal morphological behaviour from high-resolution, long-term bathymetric surveys along the Holland coast using eigenfunction analysis. Mar. Geol. 126 (1), 301–330.

Yates, M., Guza, R., O'Reilly, W., Seymour, R., 2009. Seasonal persistence of a small southern California beach fill. Coast. Eng. 56 (5–6), 559–564.